Supporting Information

Illustrating the Role of Quaternary-N of BINOL Covalent Triazine based Frameworks in Oxygen Reduction and Hydrogen Evolution Reactions

Himanshu Sekhar Jena[a*], Chidharth Krishnaraj[a], Shaikh Parwaiz[b], Florence Lecoeuvre,[a] Johannes Schmidt[c], Debabrata Pradhan[b*], Pascal Van Der Voort[a*]

[a]Center for Ordered Materials, Organometallics and Catalysis (COMOC), Department of Chemistry, Ghent University, Krijgslaan 281 (S3 B), 9000 Ghent, Belgium

[b]Materials Science Centre, Indian Institute of Technology Kharagpur, Kharagpur, West Bengal 721 302, India

[c]Technische Universität Berlin, Institut für Chemie – Funktionsmaterialien, Hardenbergstraße 40, 10623 Berlin, Germany

Corresponding Authors:

Pascal Van Der Voort (pascal.vandervoort@ugent.be)
Debabrata Pradhan (deb@matsc.iitkgp.ac.in)
Himanshu Sekhar Jena (Himanshu.jena@ugent.be ; hsjena@gmail.com)

GENERAL CTF SYNTHESIS

The linker, 2,2'-dihydroxy-[1,1'-binaphthalene]-6,6'-dicarbonitrile (BINOL-CN) was synthesized as reported in the literature. For CTF synthesis, BINOL-CN and 5/10 equivalents of $ZnCl_2$ were taken together with glass ampules and dried under vacuum for 1 h. Glass ampules with materials were then vacuum sealed and heated to desired temperatures in a Nabertherm oven in 1°C/min for 48 h. After the oven reached room temperature, black materials were removed from the ampoules and dispersed in 0.1N HCl overnight, followed by reflux in water. The process was repeated until the pH paper did not change to any color. The isolated shiny black materials were cleaned with THF by stirring overnight, filtered, washed with excess THF, and dried under vacuum at 150°C. Detail synthesis conditions, yields and CHNS details are included in Table S1 and Table S2.

Table S1. Synthetic conditions and abbreviations used for all the new BINOL-CTFs[a]

Entry	Linker: $ZnCl_2$	Temperature (°C) and 48 h	abbreviations
1	1:5	400	BINOL-CTF-5-400
2	1:10	400	BINOL- CTF-10-400
3	1:5	500	BINOL-CTF-5-500
4	1:10	500	BINOL-CTF-10-500

[a] *For safety reason, maximum of 500 mg of BINOL-CN is recommended to use for the synthesis of CTF in a small glass ampoule*

Table S2. Elemental Analysis of BINOL-CTFs

Element	Calculated (wt%)	Found (wt%)			
	BINOL-CTFs	BINOL-CTF-5-400	BINOL-CTF-10-400	BINOL-CTF-5-500	BINOL-CTF-10-500
C	78.56	83.492	84.512	84.839	84.443
H	3.60	2.665	2.519	2.176	2.274
N	8.33	2.352	1.653	2.372	**3.105**
O	9.51	6.133	5.430	4.299	4.072
N/C	0.106	0.028	0.019	0.0279	**0.036**

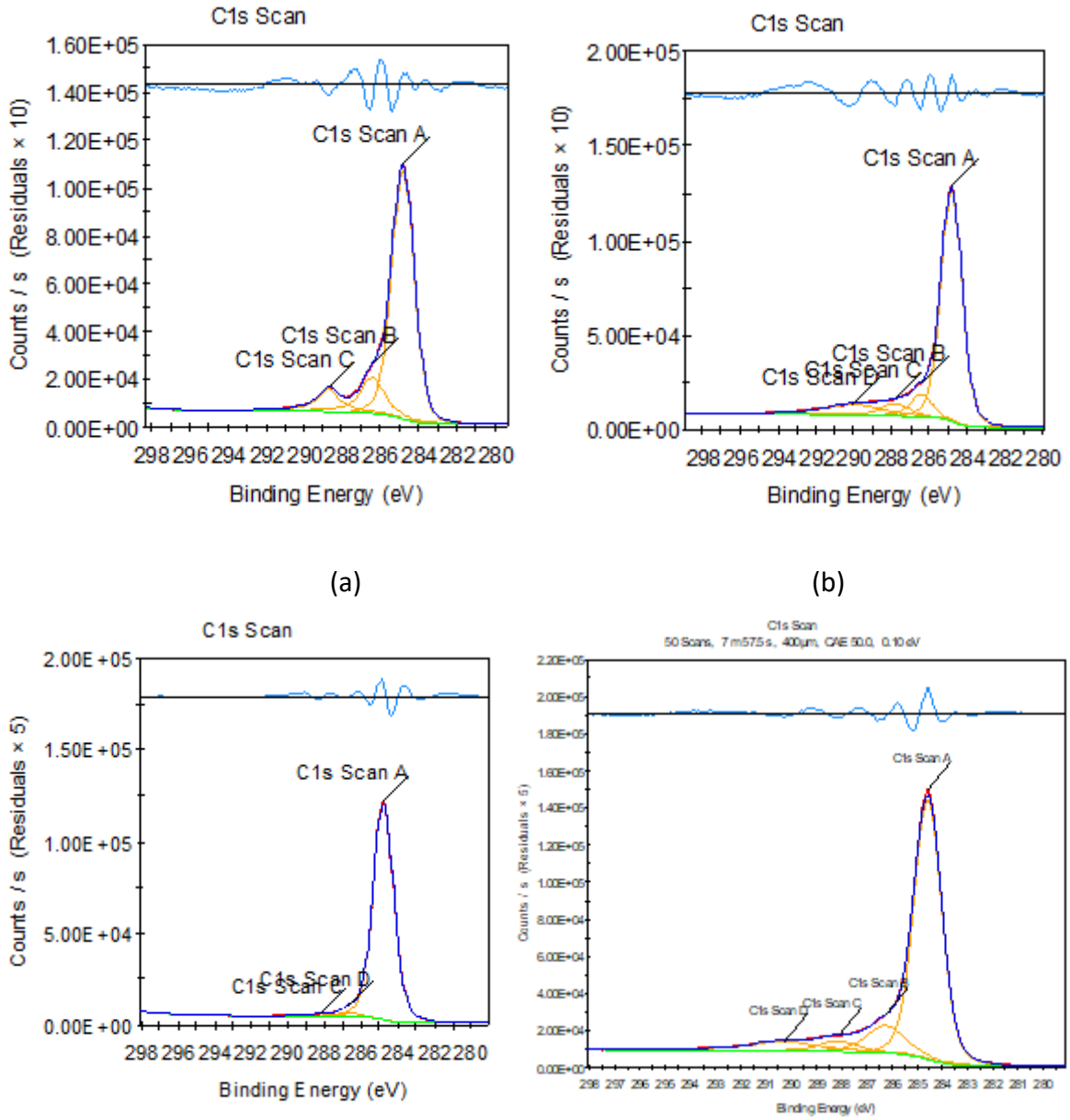

Figure S1. Deconvoluted XPS C1s spectra for (a) BINOL-CTF-5-400, (b) BINOL-CTF-10-400, (c) BINOL-CTF-5-500 and (d) BINOL-CTF-10-500

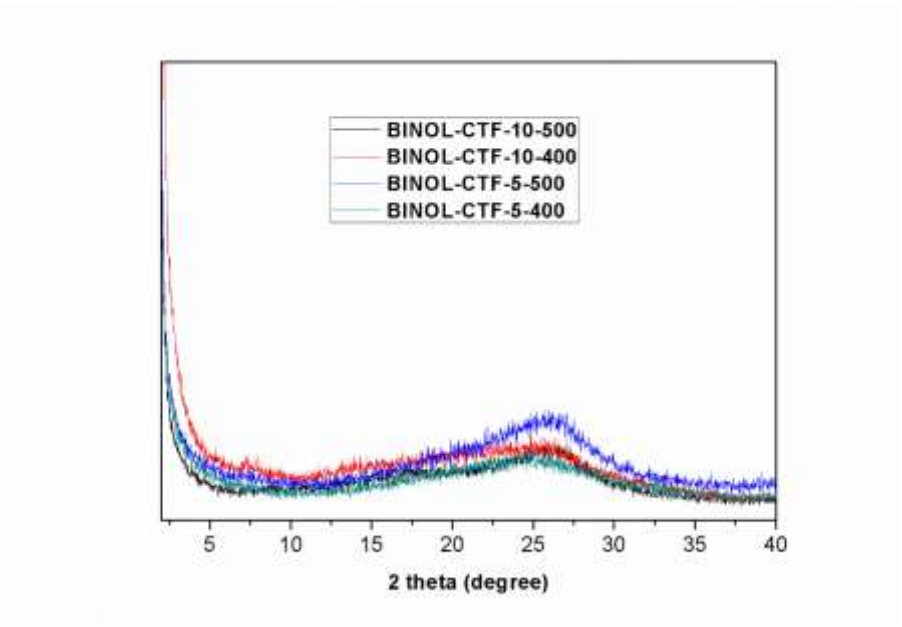

Figure S2. Powder X-ray diffraction (PXRD) spectra of all BINOL-CTFs.

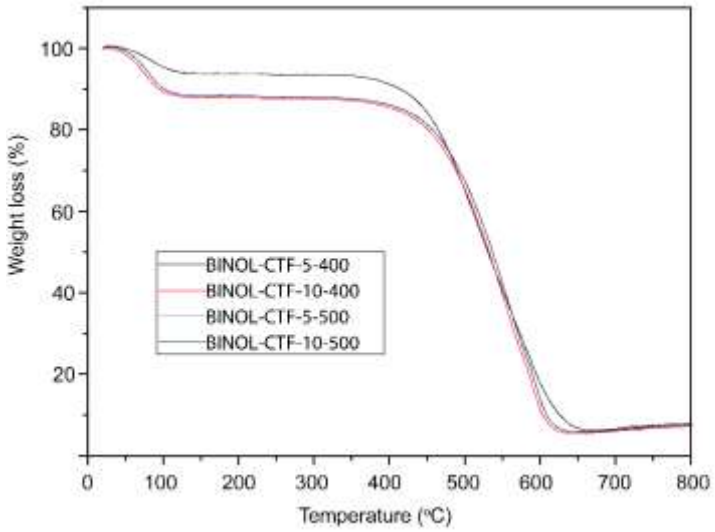

Figure S3. Thermogravimetric analysis spectra of all the BINOL-CTFs.

Discussion of gas sorption of all the BINOL-CTFs:

CO_2 adsorption/desorption isotherms were recorded at 273 K and 298 K and H_2 at 77K and at 1 bar of pressure (Figure S4 and S5). The uptake of both sets of CTF materials at respective temperatures are included in Table 1. Since only 1-3 wt% of N was obtained, these materials interact with fewer CO_2 molecules and a moderate CO_2 adsorption was therefore observed. In order to further investigate the difference in CO_2 capacities, the isosteric heats of adsorptions (Qst) of CO_2 were calculated using the Clausius-Clapeyron equation. It was observed from the obtained values (shown in Figure S6) that Q_{st} value of BINOL-CTF-10-500 is the highest of the BINOL-CTFs. This confirmed that materials with strong interactions with CO_2 molecules take up greater amounts, a finding consistent with existing literature.[1-3]

Furthermore, due to their large micropore volume, they were explored for CO2 separation from a mixture of CO_2 and N_2 gases. The selectivities are calculated using Henry's law, by taking the ratio of the initial slopes of the CO_2 (<0.06 bar) and N_2 (<0.1 bar) at 298 K (Table 1; Figure S7). The obtained values in Table 1 represent an excellent CO_2/N_2 selectivity in comparison to state-of-art CTF-based materials.[1-3] BINOL-CTF-5-400 exhibited the highest selectivity, 91, at 298 K. The obtained selectivity is directly correlated to the micro-pore volume of the materials.

We also measured H_2-storage abilities of the BINOL-CTFs at 77 K and obtained values between 0.4-0.9wt% (Figure S5). BINOL-CTF-10-500 exhibited the highest H_2 uptake of all the BINOL-CTFs, comparable with CTF materials with pyridine, bipyridine, benzimidazole, carbazole and other functional groups with similar synthesis conditions.[1]

It can thus be concluded that CTF materials with a greater amount of N exhibit highest level of CO_2 and H_2 uptake, and the materials with large micropore volume show the greatest CO_2/N_2 selectivity.

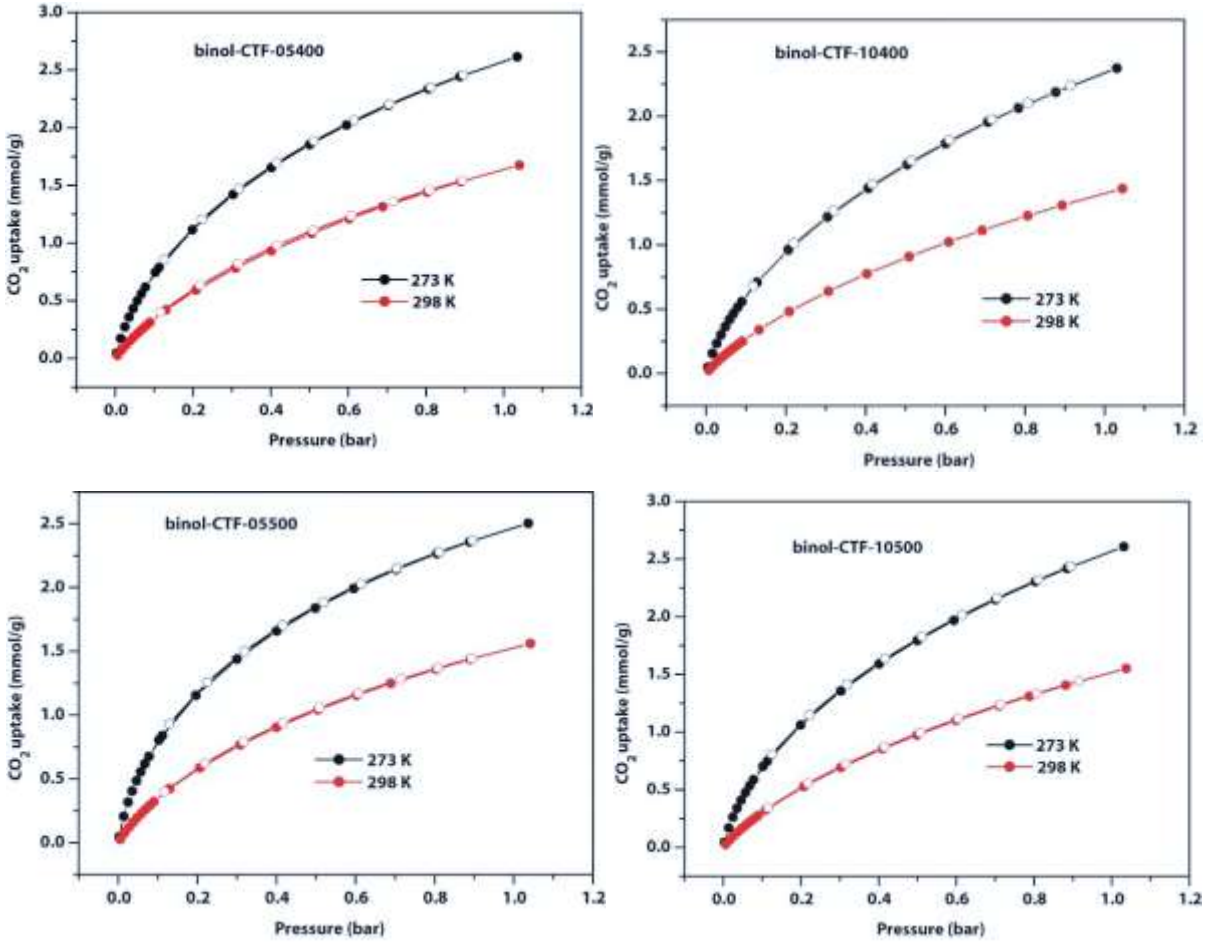

Figure S4. CO_2 adsorption/desorption isotherms all the BINOL-CTFs at 273 K and 298 K and at 1bar (filled and empty symbols represent adsorption and desorption respectively).

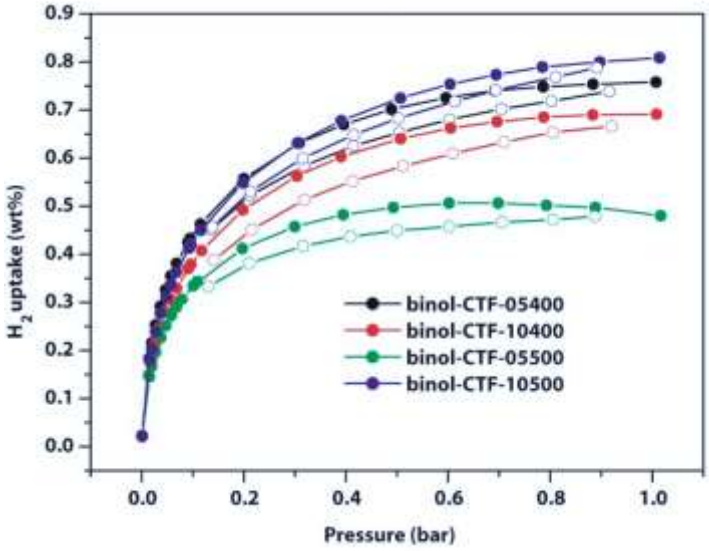

Figure S5. H_2 adsorption/desorption isotherms all the BINOL-CTFs at 77 K and at 1bar (filled and empty symbols represent adsorption and desorption respectively).

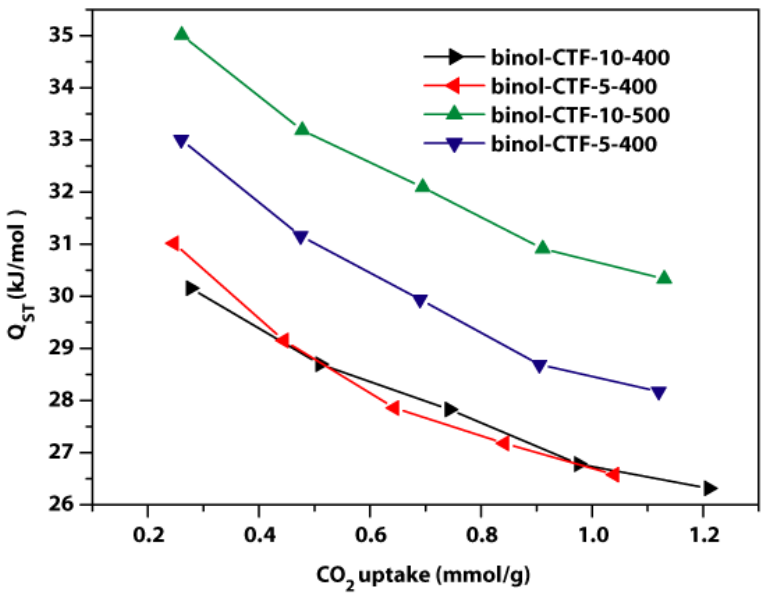

Figure S6. Isosteric heat (Qst) of CO_2 adsorption for all BINOL-CTFs.

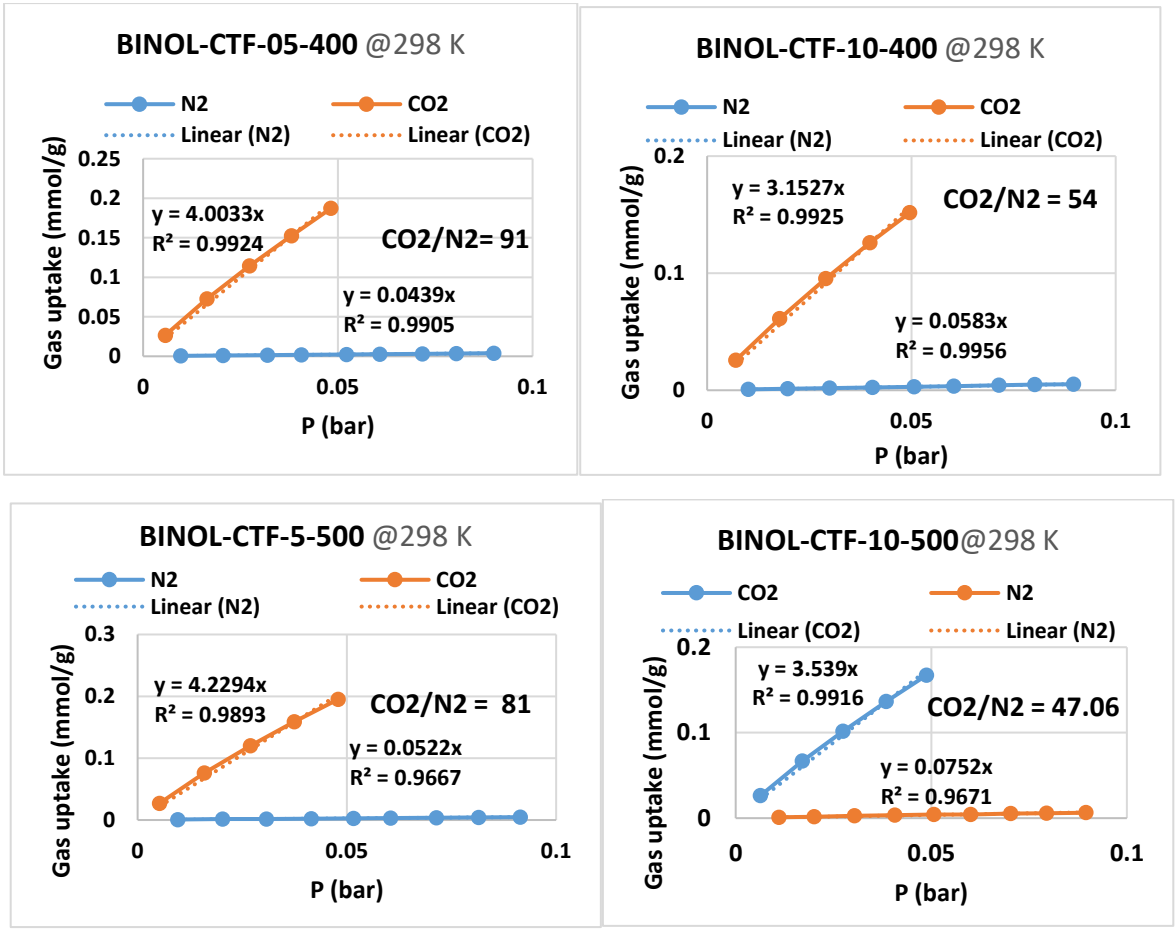

Figure S7. Henry plots of BINOL-CTFs as obtained from CO_2 and N_2 isotherms at 298K.

Electrochemical study. All the electrochemical measurements were performed in a conventional three-electrode system using a CHI 760D electrochemical workstation (CH Instruments, Inc., USA). Here, modified rotating disk electrode (RDE), Pt wire, and saturated calomel electrode (SCE) were used as working, counter, and reference electrode, respectively. The modified RDE was prepared by drop casting slurry of the synthesized electrocatalyst material on a pre-cleaned RDE electrode. The slurry was prepared by ultrasonically dispersing 5 mg of the as-synthesized electrocatalyst in 1 mL of isopropanol with 20 µL of 5% Nafion solution for 1 h. 80 µL of slurry was drop casted on RDE.

SCE to RHE conversion.

All potentials in RHE scale was obtained from SCE scale using Nernst equation:
$E_{RHE} = E_{SCE} + 0.0591 \times pH + E^{\circ}_{SCE}$
Here, E_{SCE} is the measured potential and $E^{\circ}_{SCE} = 0.2444$ V.
In alkaline environment (0.1 M KOH for ORR catalysis),
$E_{RHE} = E_{SCE} + 0.0591 \times 13 + 0.2444 = E_{SCE} + 1.0127$ V
In acid environment (0.5 M H_2SO_4 for HER catalysis),
$E_{RHE} = E_{SCE} + 0.0591 \times 0 + 0.2444 = E_{SCE} + 0.2444$ V

Oxygen reduction reaction (ORR) study. For ORR catalysis measurements, the cyclic voltammograms (CVs) were recorded in O_2 saturated 0.1 M KOH in the potential window of −0.8 to 0.2 V at different scan rates. Linear sweep voltammetry (LSV) was performed in O_2 saturated 0.1 M KOH solution at different RDE rotation speeds. The electrochemical impedance spectroscopy (EIS) study was carried out with the catalyst modified RDE in 0.1 M KOH electrolytic solution in a frequency range of 1 MHz to 100 Hz with a sinusoidal perturbation of 2 mV. For comparison, the electrocatalytic performance of commercial 10 wt % Pt/C catalyst was also investigated under the same conditions.

Determination of electron transfer number and kinetic current density from K-L plots (ORR catalysis).

The electron transfer numbers per O_2 in the ORR process was calculated by Koutecky–Levich (K–L) equation (equation 1) as stated below.[4]

$$\frac{1}{J} = \frac{1}{J_k} + \frac{1}{J_l} = \frac{1}{J_k} + \frac{1}{B\omega^{0.5}} \qquad (1)$$

where, J is the measured current density, J_k is the kinetic current density, J_l is the diffusion-limiting current density, ω is the rotation speed of electrode expressed in rpm. The corresponding K-L plot was obtained from J^{-1} vs. $\omega^{-0.5}$ plot (Figure 5c, Figure S9b, Figure S10(a1-c1), where slope and intercept was equal to B^{-1} and J_k^{-1}, respectively. According to Levich equation (equation 2),

$$B = 0.2nFC_{O_2}D_{O_2}^{\frac{2}{3}}\upsilon^{\frac{-1}{6}} \qquad (2)$$

where, n is the number of electron transferred per oxygen molecule, F is the faraday constant (96485 C mol^{-1}), C_{O_2} is the bulk concentration of O_2 (2.4×10^{-7} mol cm^{-3}), υ is the kinematic viscosity of the electrolyte (0.01 $cm^2 S^{-1}$). D_{O_2} is the diffusion coefficient of O_2 in 0.1 M KOH (1.73×10^{-5} $cm^2 S^{-1}$). The constant 0.2 was taken as rotation speed is quoted in rpm. By using Levich equation and taking n = 4 for Pt, the number of electron transferred for ORR with 5400, 5500, 10400, and 10500 was found to be 1.86, 2.57, 1.99, and 4.04 respectively. The n value obtained for 10500 clearly suggest it's near four electrons ORR kinetics with least possible formation of hydrogen peroxide.

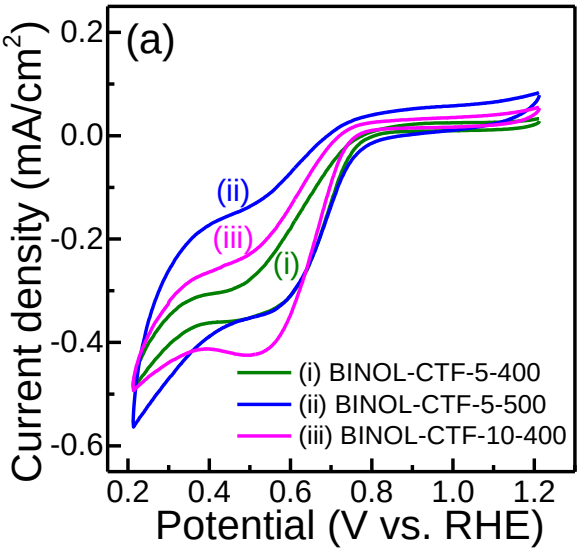

Figure S8. CV profiles of other BINOL-CTFs at 10 mV/s.

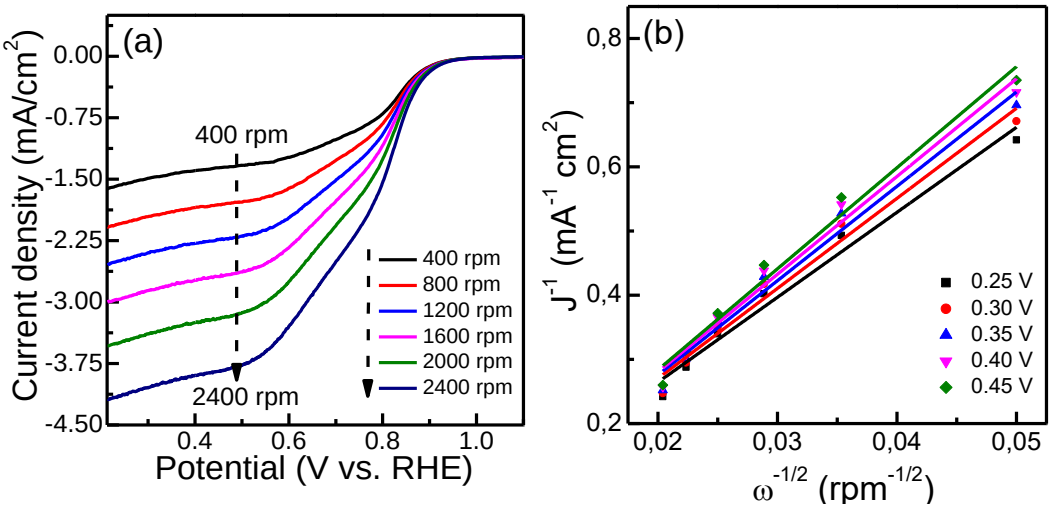

Figure S9. (a) LSV plots of Pt/C in O_2 saturated 0.1 M KOH at different RDE rotation speeds and (b) corresponding K-L plots.

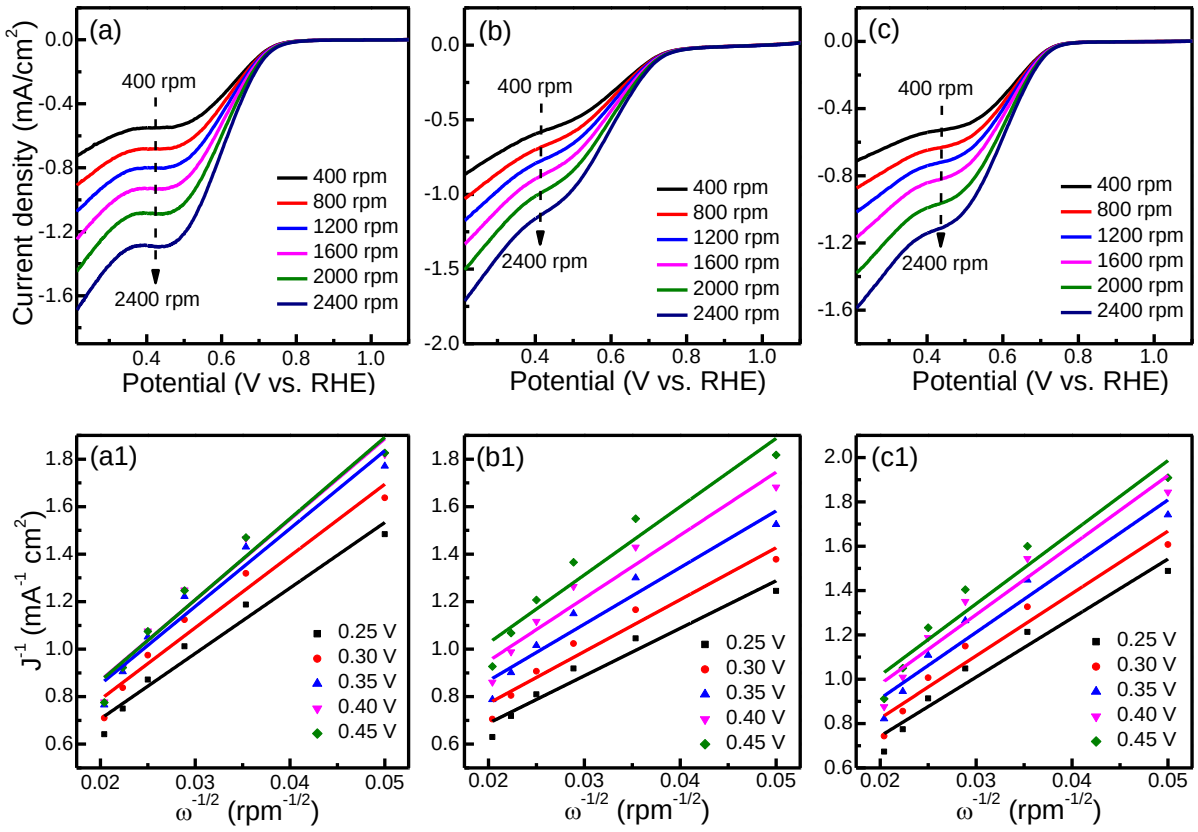

Figure S10. LSV plots of (a) BINOL-CTF-5-400, (b) BINOL-CTF-5-500, and (c) BINOL-CTF-10-400 in O_2 saturated 0.1 M KOH at different RDE rotation speeds and (a1-c1) corresponding K-L plots.

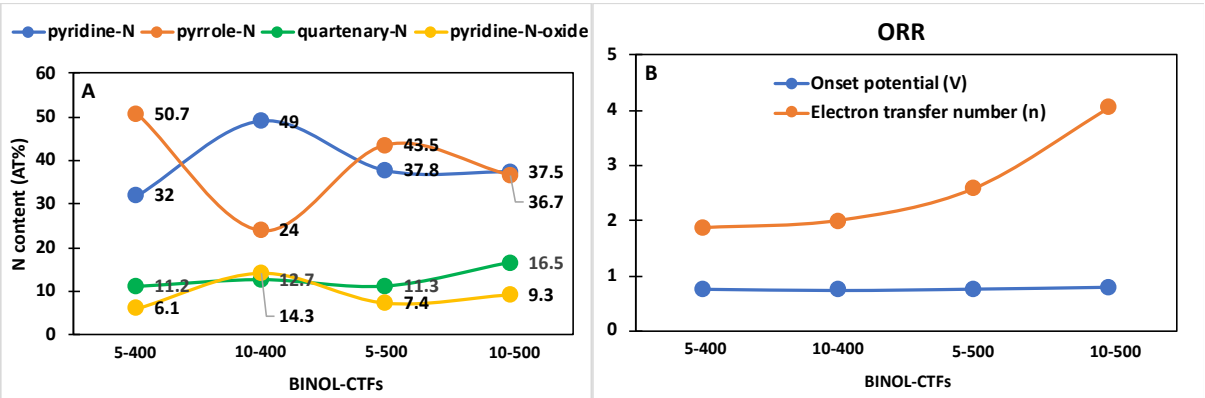

Figure S11. (A) The change in relative amount of pyridinic-N, pyrrolic-N, quaternary-N and pyridine-N-oxide in each BINOL-CTFs and (B) the respective change in the onset potential and electron transfer number in ORR

Table S3. ORR onset potential, half-wave potential, and electron transfer number of synthesized electrocatalysts obtained from CV, LSV, and EIS study.

Sample Name	Onset Potential (V)	Half-wave Potential (V)	Electron transfer number (n) (at 0.3 V)	Charge transfer resistance (Ω)
BINOL-CTF-5-400	0.758	0.684	1.86	54.86
BINOL-CTF-5-500	0.760	0.688	2.57	59.5
BINOL-CTF-10-400	0.737	0.659	1.99	60.27
BINOL-CTF-**10-500**	**0.793**	**0.737**	**4.04**	**56.6**
Pt/C	0.940	0.880	4	62.98

Table S4. Metal-free heteroatom doped carbon catalysts for oxygen reduction reaction.

Electrocatalyst	Onset potential (mV)	Half-wave potential (mV)	Electron transfer number	Electrolyte	Reference
BINOL-CTF-10-500	**793**	**737**	**4.0**	**0.1 M KOH**	**This work**
CTF/CPs	810	-	3.95	Phosphate buffer solution	[5]
CuS-CTF/CP	880	-	-	Phosphate buffer solution	[6]
NHC-rGO-950	950	830	3.91	0.1 M KOH	[7]
TETCB-Fe-N/S/C	899	790		0.1 M $HClO_4$	[8]
TTF-F	860	767	3.9	0.1 M KOH	[9]
CTF-CSU1	790	570	2.6	0.1 M KOH	[10]
CTF-Super P-10	981	883	4.01	0.1 M KOH	[11]
N-GNS-1	770	-	-	0.1 M H_2SO_4	[12]
NPC-0	820	730	3.23	0.1 M KOH	[13]
NCS-800	725	-	3.98	0.5 M H_2SO_4	[14]
Carbon-L	860	700	3.68	0.1 M KOH	[15]
N:C-MgNTA	890	750	4.28	0.1 M KOH	[16]
NC900	830	-	3.3	0.1 M KOH	[17]
C-COP-4	-	780	3.9	0.1 M KOH	[18]
N-CNF aerogel	-	800	3.96	0.1 M KOH	[19]
N,P-GCNS	1010	850	3.96	0.1 M KOH	[20]
NC-900	972	855	3.98	0.1 M KOH	[21]

Hydrogen evolution reaction (HER) study. For HER study, the LSVs were recorded in N_2 saturated 0.5 M H_2SO_4 solution in the potential window of −0.8 to 0.2 V with a scan rate of 10 mV/s at constant RDE rotation speed of 1600 rpm. The EIS study was carried out with the catalyst modified RDE in 0.5 M H_2SO_4 electrolytic solution in a frequency range of 0.5 MHz to 100 Hz with a sinusoidal perturbation of 5 mV. For comparison, the electrocatalytic performance of commercial 10 wt % Pt/C catalyst was also investigated under the same conditions.

Table S5. HER onset potential, potential at 10 mA cm^{-2}, Tafel slope, double layer capacitance, electrochemical active surface area, and charge transfer resistance of synthesized electrocatalysts.

Sample Name	Onset Potential (mV)	Potential at 10 mA cm^{-2} (mV)	Tafel slope (mV/dec)	Double layer capacitance (μF)	ECSA (cm^2)	Charge transfer resistance (Ω)
BINOL-CTF-5-400	−110	−392	180.15	227.54	5.688575	20.75
BINOL-CTF-5-500	−120	−463	64.79	79.94	1.9985725	19.5
BINOL-CTF-10-400	−71	−371	55.24	142.83	3.570725	18.34
BINOL-CTF-**10-500**	**−66**	**−311**	**41.04**	**469**	**11.725**	**10.98**
Pt/C	−62	−89	31.12	-	-	17.43

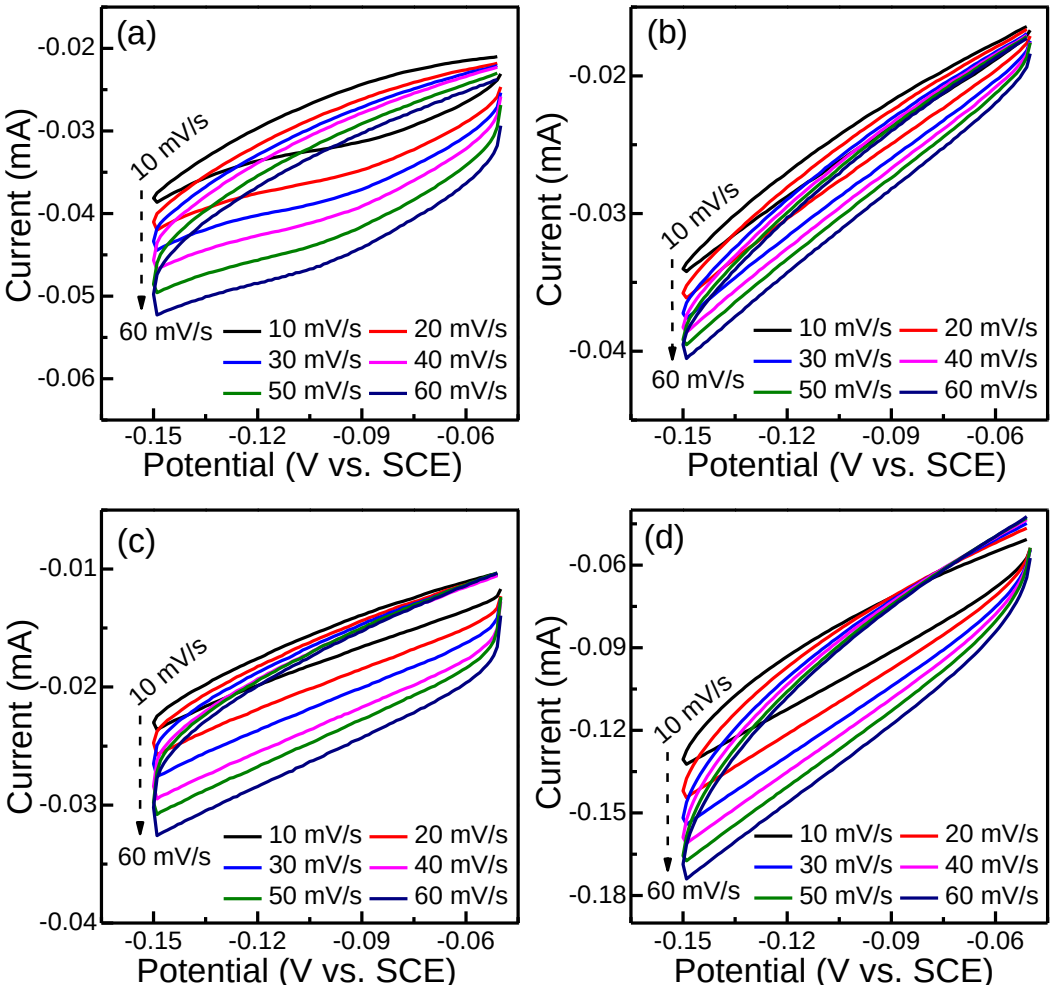

Figure S12. CV plots of (a) BINOL-CTF-5-400, (b) BINOL-CTF-5-500, (c) BINOL-CTF-10-400, and (d) BINOL-CTF-10-500 at different scan rates with RDE rotation speed of 1600 rpm in N_2 saturated 0.5 M H_2SO_4 respectively.

References

1. Krishnaraj, C.; Jena, H. S.; Leus, K.; Van Der Voort, P., Covalent triazine frameworks – a sustainable perspective. *Green Chem.,* **2020,** *22* (4), 1038-1071.
2. Liu, M.; Guo, L.; Jin, S.; Tan, B., Covalent triazine frameworks: synthesis and applications. *J. Mater. Chem. A* **2019,** *7* (10), 5153-5172.
3. Puthiaraj, P.; Lee, Y.-R.; Zhang, S.; Ahn, W.-S., Triazine-based covalent organic polymers: design, synthesis and applications in heterogeneous catalysis. *J. Mater. Chem. A* **2016,** *4* (42), 16288-16311.
4. Qu, L.; Liu, Y.; Baek, J.-B.; Dai, L., Nitrogen-doped graphene as efficient metal-free electrocatalyst for oxygen reduction in fuel cells. *ACS Nano* **2010,** *4* (3), 1321-1326.
5. Iwase, K.; Yoshioka, T.; Nakanishi, S.; Hashimoto, K.; Kamiya, K., Copper-Modified Covalent Triazine Frameworks as Non-Noble-Metal Electrocatalysts for Oxygen Reduction. *Angew. Chem. Int. Ed.* **2015,** *54* (38), 11068-11072.
6. Iwase, K.; Kamiya, K.; Miyayama, M.; Hashimoto, K.; Nakanishi, S., Sulfur-Linked Covalent Triazine Frameworks Doped with Coordinatively Unsaturated Cu(I) as Electrocatalysts for Oxygen Reduction. *ChemElectroChem* **2018,** *5* (5), 805-810.
7. Jiao, L.; Hu, Y.; Ju, H.; Wang, C.; Gao, M.-R.; Yang, Q.; Zhu, J.; Yu, S.-H.; Jiang, H.-L., From covalent triazine-based frameworks to N-doped porous carbon/reduced graphene oxide nanosheets: efficient electrocatalysts for oxygen reduction. *J. Mater. Chem. A* **2017,** *5* (44), 23170-23178.
8. Zhu, Y.; Chen, X.; Liu, J.; Zhang, J.; Xu, D.; Peng, W.; Li, Y.; Zhang, G.; Zhang, F.; Fan, X., Rational Design of Fe/N/S-Doped Nanoporous Carbon Catalysts from Covalent Triazine Frameworks for Efficient Oxygen Reduction. *ChemSusChem* **2018,** *11* (14), 2402-2409.
9. Hao, L.; Zhang, S.; Liu, R.; Ning, J.; Zhang, G.; Zhi, L., Bottom-Up Construction of Triazine-Based Frameworks as Metal-Free Electrocatalysts for Oxygen Reduction Reaction. *Adv. Mater.,* **2015,** *27* (20), 3190-3195.
10. Yu, W.; Gu, S.; Fu, Y.; Xiong, S.; Pan, C.; Liu, Y.; Yu, G., Carbazole-decorated covalent triazine frameworks: Novel nonmetal catalysts for carbon dioxide fixation and oxygen reduction reaction. *J. Catal.,* **2018,** *362*, 1-9.
11. Cao, Y.; Zhu, Y.; Chen, X.; Abraha, B. S.; Peng, W.; Li, Y.; Zhang, G.; Zhang, F.; Fan, X., N-doped hierarchical porous metal-free catalysts derived from covalent triazine frameworks for the efficient oxygen reduction reaction. *Catal. Sci. Technol.,* **2019,** *9* (23), 6606-6612.
12. Guo, D.; Shibuya, R.; Akiba, C.; Saji, S.; Kondo, T.; Nakamura, J., Active Sites in Nitrogen-Doped Carbon Materials for Oxygen Reduction Reaction clarified using model catalysts. *Science* **2016,** *351* (6271), 361-365
13. Liu, Z.; Zhang, G.; Lu, Z.; Jin, X.; Chang, Z.; Sun, X., One-step scalable preparation of N-doped nanoporous carbon as a high-performance electrocatalyst for the oxygen reduction reaction. *Nano Res.,* **2013,** *6* (4), 293-301.
14. Chen, P.; Wang, L.-K.; Wang, G.; Gao, M.-R.; Ge, J.; Yuan, W.-J.; Shen, Y.-H.; Xie, A.-J.; Yu, S.-H., Nitrogen-doped nanoporous carbon nanosheets derived from plant biomass: an efficient catalyst for oxygen reduction reaction. *Energy Environ. Sci.,* **2014,** *7* (12), 4095-4103.
15. Zhang, P.; Sun, F.; Xiang, Z.; Shen, Z.; Yun, J.; Cao, D., ZIF-derived in situ nitrogen-doped porous carbons as efficient metal-free electrocatalysts for oxygen reduction reaction. *Energy Environ. Sci.,* **2014,** *7* (1), 442-450.
16. Eisenberg, D.; Stroek, W.; Geels, N. J.; Sandu, C. S.; Heller, A.; Yan, N.; Rothenberg, G., A Simple Synthesis of an N-Doped Carbon ORR Catalyst: Hierarchical Micro/Meso/Macro Porosity and Graphitic Shells. *Chem. Euro. J.,* **2016,** *22* (2), 501-505.
17. Aijaz, A.; Fujiwara, N.; Xu, Q., From metal–organic framework to nitrogen-decorated nanoporous carbons: high CO2 uptake and efficient catalytic oxygen reduction. *J. Am. Chem. Soc.* **2014,** *136* (19), 6790-6793.
18. Xiang, Z.; Cao, D.; Huang, L.; Shui, J.; Wang, M.; Dai, L., Nitrogen-doped holey graphitic carbon from 2D covalent organic polymers for oxygen reduction. *Adv. Mater.* **2014,** *26* (20), 3315-3320.

19. Liang, H.-W.; Wu, Z.-Y.; Chen, L.-F.; Li, C.; Yu, S.-H., Bacterial cellulose derived nitrogen-doped carbon nanofiber aerogel: An efficient metal-free oxygen reduction electrocatalyst for zinc-air battery. *Nano Energy* **2015,** *11*, 366-376.
20. Li, R.; Wei, Z.; Gou, X., Nitrogen and Phosphorus Dual-Doped Graphene/Carbon Nanosheets as Bifunctional Electrocatalysts for Oxygen Reduction and Evolution. *ACS Catal.,* **2015,** *5* (7), 4133-4142.
21. Yang, M.; Liu, Y.; Chen, H.; Yang, D.; Li, H., Porous N-Doped Carbon Prepared from Triazine-Based Polypyrrole Network: A Highly Efficient Metal-Free Catalyst for Oxygen Reduction Reaction in Alkaline Electrolytes. *ACS Appl. Mater. Interfaces* **2016,** *8* (42), 28615-28623.